Hindawi
Mathematical Problems in Engineering
Volume 2018, Article ID 8052415, 11 pages
https://doi.org/10.1155/2018/8052415

Research Article

An RSSD-Based Fingerprint Positioning Method for Detection of an Unknown Radio Transmitter Using WLS and Factor Graph

Liyang Zhang, Taihang Du, and Chundong Jiang

The School of Control Science and Engineering, Hebei University of Technology, Tianjin, 300130, China

Correspondence should be addressed to Taihang Du; thdu@hebut.edu.cn

Received 26 September 2018; Accepted 17 December 2018; Published 30 December 2018

Academic Editor: Paolo Addesso

Realizing accurate detection of an unknown radio transmitter (URT) has become a challenge problem due to its unknown parameter information. A method based on received signal strength difference (RSSD) fingerprint positioning technique and using factor graph (FG) has been successfully developed to achieve the localization of an URT. However, the RSSD-based FG model is not accurate enough to express the relationship between the RSSD and the corresponding location coordinates since the RSSD variances of reference points are different in practice. This paper proposes an enhanced RSSD-based FG algorithm using weighted least square (WLS) to effectively reduce the impact of RSSD measurement variance difference on positioning accuracy. By the use of stochastic RSSD errors between the measured value and the estimated value of the selected reference points, we utilize the error weight matrix to establish a new WLSFG model. Then, the positioning process of proposed RSSD-WLSFG algorithm is derived with the sum-product principle. In addition, the paper also explores the effects of different access point (AP) numbers and grid distances on positioning accuracy. The simulation experiment results show that the proposed algorithm can obtain the best positioning performance compared with the conventional RSSD-based K nearest neighbor (RSSD-KNN) and RSSD-FG algorithms in the case of different AP numbers and grid distances.

1. Introduction

Currently, a variety of radio signals have been widely used and existed in our daily life. To strengthen the monitoring of illegal radio spectrum resources, protect the rights and interests of legitimate users, and combat the occupation of illegal signal resources are related to the security and privacy of the nation, enterprises, and individuals. A challenging issue that realizes the accurate detection of an unknown radio transmitter (URT) is a crucial work in radio management.

At present, most of the positioning techniques for the URT are developed based on the measurements obtained by access point (AP). The measurements mainly include time difference of arrival (TDOA) [1], frequency different of arrival (FDOA) [2], received signal strength (RSS) [3, 4], angle of arrival (AOA) [5], and hybrid of them [6, 7]. Among all the measurements, the RSS-based fingerprint positioning technique is widely used for its characteristics of no extra antenna arrays, no time synchronization limitation, and low cost. The process of RSS-based fingerprint positioning method is mainly divided into two phases, i.e., the offline database establishment phase and the online positioning phase. In the offline database establishment phase, the RSS measurements are collected from different access points (APs) deployed in the positioning area. Then, the RSS and corresponding location coordinates construct the offline fingerprint database. In the online positioning phase, the positioning target location is estimated by collecting the real-time RSS measurements and matching the fingerprint database with the appropriate positioning algorithm. Two typical RSS-based fingerprint positioning techniques using K nearest neighbor (KNN) [8] method are RADAR [9] abbreviated as the 4NN algorithm and LANDMARC [10], respectively. The basic principle of KNN is calculating the location of positioning target by averaging locations of K reference points with the minimum Euclidean distance found in the fingerprint database. However, the RSS-based fingerprint positioning techniques are very difficult to accurately detect the URT since the transmit power of URT is unknown. After that, a robust fingerprint approach based on received signal strength difference (RSSD)

is first proposed to eliminate the influence caused by the hardware variations of the radio transmitter in the offline phase and online phase [11]. Reference [12] presents a cooperative location algorithm based on RSSD/TDOA, which is suitable for the application scenarios that the priori knowledge is unknown such as transmit power and signal transmission instantaneous time of the primary user.

Among all positioning algorithms, the technique based on factor graph (FG) is famous for the low computational complexity and high positioning accuracy. Many kinds of FG positioning techniques based on the various measurements described above have been developed in recent years. The TOA-FG [13, 14] technique uses the time of signal propagation between the radio transmitter and APs to estimate the distance, but it requires the clocks of both to be synchronous. In order to be free from the limitation of clock synchronization between the radio transmitter and the APs, a TDOA-FG technique utilizing hyperbolic approach is proposed in [15]. In addition, [16] presents another Pythagorean TDOA-based FG (PTDOA-FG) technique. It should be noted that the radio transmitter and APs also need to be synchronized with the clock of the reference node. However, TOA-based FG and TDOA-based FG methods are both more suitable for line of sight (LOS) positioning scenario. The RSS-FG [17] technique overcomes the requirement of clock synchronization and establishes the mathematical relationship between the RSS measurements and corresponding location coordinates. Moreover, RSS information contains the result information caused by the influence of environment and device hardware, and it is also suitable for LOS and nonline of sight (NLOS) positioning environment. Yet, the RSS-FG technique has been proved to be inapplicable to the precise localization of URT, because we cannot obtain the transmission frequency and power of the unknown signal source in advance. Reference [18] proposes an RSSD-FG technique to realize the detection of an URT. Moreover, it can also mitigate the influence caused by hardware variations of the URT. However, the mathematical model established in the RSSD-FG algorithm is not accurate enough, because the model considers that the RSSD measurement variance of each selected reference point is the same and ignores the difference of the RSS measurement variances among the selected reference points. Thus, the selected reference points with large RSSD measurement variance have a great impact on the model accuracy, which results in reducing the positioning accuracy.

In this paper, we combine the RSSD-based FG fingerprint positioning technique and weighted least square (WLS) method to propose the RSSD-WLSFG algorithm. A more accurate RSSD-based WLSFG model is constructed to express the relationship between RSSD measurement and the corresponding location coordinates. Different from the RSSD-FG following RSS-FG to calculate the coefficients of linear equation between the location coordinates and RSSD by the use of least square (LS), this paper utilizes the stochastic RSSD errors between the measured value and the estimated value of the selected reference points to construct the error weight matrix and obtains the coefficients with the WLS method. In this way, it can reduce the influence of the selected reference points with larger measurement variance so as to achieve a more accurate model. The proposed RSSD-WLSFG positioning system for detecting an URT is as shown in Figure 1. Four APs are used as an example to express the proposed method in our work. At first, the APs are deployed with a certain location in the positioning area. The positioning area is divided into a lot of grid areas with side length d. The vertices of the grid areas are defined as the reference points, and d is denoted as grid distance. Second, we select a known radio transmitter to traverse each reference point and record the RSS measurements by different APs. Then, the processed RSSD and corresponding location coordinates of reference points are stored in the offline fingerprint database. Finally, when an URT as positioning target enters the positioning area, its real-time RSS measurements will be collected and uploaded to the computer server. The computer server converts the RSSD measurements to the location coordinates of the positioning target by using the factor graph and sum-product algorithm. The soft-information of factor graph is transported between the variable nodes and the factor nodes until the estimated location of positioning target is obtained.

In our research, the proposed RSSD-WLSFG technique is considered to be an effective method for detecting an URT. The main benefits are briefly summarized as follows: (1) the complex problem can be converted into subproblems with a set of fewer local variables. (2) The RSS measurements are processed with mean and variance in the form of Gaussian distribution. (3) A more accurate mathematical model between RSSD and location coordinates is established by WLS method to reduce the impact of differences in variance of RSSD at different reference points on positioning accuracy.

The rest of the paper is organized as follows. We introduce the factor graph and sum-product algorithm and the RSSD-FG model in Section 2. Next, the proposed RSSD-WLSFG algorithm and detailed iteration process are derived in Section 3. In Sections 4 and 5, the positioning performance of RSSD-WLSFG is compared with the conventional 4NN method using the RSSD information (RSSD-4NN) and RSSD-FG algorithm by numerous simulation experiments.

2. The Algorithm and System Model

In this section, we express that the factor graph and sum-product algorithm are used to efficiently process the RSS measurements to realize the localization of an URT. The main idea of factor graph and sum-product algorithm is briefly summarize as in [19]. Then, an RSSD-based FG model is established with this method. In the following subsection, we introduce the spirit of factor graph and sum-product principle at first.

2.1. Factor Graph and Sum-Product Algorithm. A factor graph is a bidirectional graph that describes how to decompose a multivariate global function into the product of multiple local functions. On the basis of the factor graph, the sum-product algorithm is developed to calculate the edge distribution of global functions by soft-information transmission in the

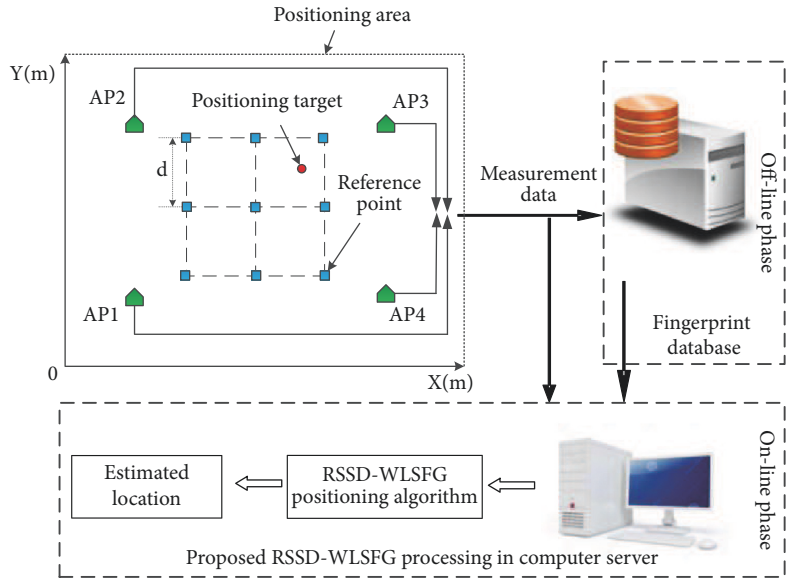

Figure 1: Structure of proposed RSSD-WLSFG positioning system with 4 APs and an URT.

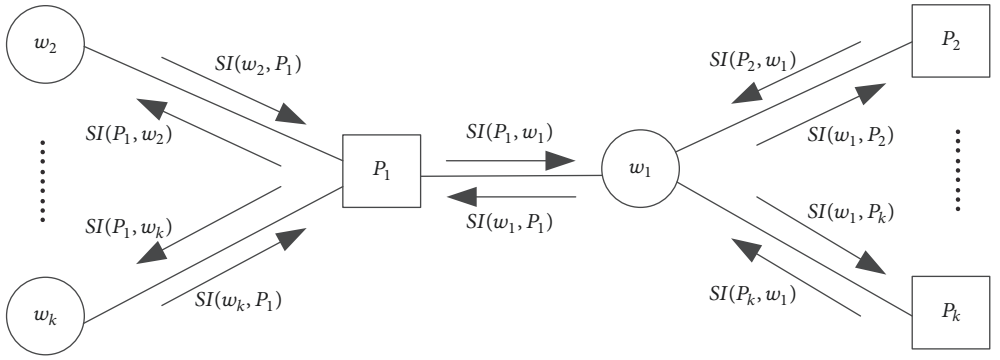

Figure 2: Fragment of a factor graph showing the soft-information transported rules of sum-product algorithm.

corresponding graph model. In general, a factor graph model consists of the variable nodes $(w_1, \ldots, w_k)$ and the factor nodes $(P_1, \ldots, P_k)$ as shown in Figure 2. The factor node P_k represents the local function node in related to the variable node w_k. Considering the fragment of factor graphs shown in Figure 2, the factor nodes can be separated with joint distribution into groups. Here, the problem of calculating local functions can be solved by using the sum-product algorithm. The sum-product algorithm works by collecting the soft-information transmission of local function product along the path in the factor graph. The soft-information transported between the variable nodes and the factor nodes represents the stochastic properties of the associated variable nodes. With several iteration processes of soft-information transported between the variable nodes and the factor nodes, the solution of variables to a problem expressed by a factor graph can be easily obtained.

In this paper, we denote $SI(a, b)$ being the soft-information transported from node a to node b, which represents the statistical properties of the variable nodes and measurement errors in the form of a Gaussian probability density function $(SI(a, b) \sim N(m_{a,b}, \sigma^2_{a,b}))$. The mean and variance of $SI(a, b)$ are $m_{a,b}$ and $\sigma^2_{a,b}$, respectively. For example, the soft-information transported from w_1 to P_1 can be expressed by

$$SI(w_1, P_1) = \prod_{t=2}^{k} SI(P_t, w_1), \tag{1}$$

where k is the index number of nodes. The product of some independent Gaussian distributions is still a Gaussian distribution. The mean and variance of $SI(w_1, P_1)$ can be obtained by

$$m_{w_1,P_1} = \sigma^2_{w_1,P_1} \cdot \sum_{t=2}^{k} \frac{m_{P_t,w_1}}{\sigma^2_{P_t,w_1}}, \tag{2}$$

$$\sigma^2_{w_1,P_1} = \frac{1}{\sum_{t=2}^{k} \left(1/\sigma^2_{P_t,w_1}\right)}. \tag{3}$$

The soft-information transported from the factor node to a variable node can be calculated from the product of a

local function associated with the factor node and all the soft-information of the other variable nodes as

$$SI\left(P_1, w_1\right) = \int_{w_2} \cdots \int_{w_k} \left[f\left(w_1, \ldots, w_k\right) \cdot \prod_{t=2}^{k} SI\left(P_t, w_1\right) \right] d_{w_2} \cdots d_{w_k}, \tag{4}$$

where $f(w_1, \ldots, w_k)$ is the location function of factor node P_1 associated with all the variable nodes. With the above sum-product update rules of (1)–(4), the variable node can be estimated through all the soft-information conveyed by the corresponding factor nodes. Thus, we can calculate the whole soft-information of w_1 with this method as follows:

$$SI\left(w_1\right) = \prod_{t=1}^{k} SI\left(P_t, w_1\right). \tag{5}$$

2.2. RSSD-Based Factor Graph System Model. The RSSD-FG technique was first introduced to detect an URT in [18] and the RSSD-based FG model is as shown in Figure 3. The proposed RSSD-based FG model also consists of two kinds of nodes, the factor nodes (H_1, H_2, H_i, G_1, G_2, G_i, P_1, P_2, and P_i) and the variable nodes (p_1, p_2, p_i, R_1, R_2, R_i, x, and y), where i is the index number of AP ($i = 1, 2, \ldots, n$) and n is the AP number. First, RSS measurements of different APs are used as the input measurements ($\widehat{p}_1$, $\widehat{p}_2$,..., $\widehat{p}_i$). When an URT enters the positioning area, AP will collect RSS measurements and they can be expressed as

$$\widehat{p}_{w,i} = \widetilde{p}_{w,i} + e_i, \tag{6}$$

where $\widetilde{p}_{w,i}$ is the RSS error-free measurement of RSS in units of watt (W) and it can be obtained by averaging some sampling values with data filtering. e_i represents the measurement error and it can be expressed by zero-mean Gaussian distribution ($e_i \sim N(0, \sigma_i^2)$). In order to better reflect the local linearity characteristic of RSS, it is processed in logarithmic scale, where $\widehat{p}_i = 10 \cdot \log_{10}(\widetilde{p}_{w,i} + e_i)$. The logarithmic RSS measurement distribution is proved to be Gaussian approximation in [17]. Factor node P_i utilizes the logarithmic RSS measurement and variance of RSS measurements to generate the variable node p_i with Gaussian distribution ($p_i \sim N(\widetilde{p}_i, \sigma_{p_i}^2)$), where $\widetilde{p}_i$ and $\sigma_{p_i}^2$ are the mean and variance of sampling logarithmic RSS, respectively. Factor node D_i represents the subtraction relationship of two different APs, in which combination is "12, 23, ..., i1." Taking an example of R_1, it can be calculated by

$$R_1 = p_1 - p_2. \tag{7}$$

In the same way, $R_2 = p_2 - p_3$, $R_3 = p_3 - p_4$, ..., and $R_i = p_i - p_1$ can be obtained and i is also the index number of AP combination. Second, factor nodes transport the soft-information from the variable nodes by using the simple local functions. Finally, the root variable nodes x and y combine with the soft-information of all the connected factor nodes based on the sum-product algorithm. Thus, the location of URT will be estimated with a few iteration processes among the source factor nodes and variable nodes.

As known from the log-normal shadowing model, the RSS measurement is related to the distance from AP. Thus, the relationship of variable nodes between the location coordinate (x, y) and logarithmic RSSD (R) can be formulated with a hyperplane equation [18], which can be expressed by

$$k_x x + k_y y + k_p R = c, \tag{8}$$

where k_x, k_y, and k_p are the coefficients and c is a nonzero constant set to one. To obtain the coefficients of (8), we need four different equations and utilize least square (LS) approach as in [18]. In this paper, four reference points are selected by using RSSD-4NN technique and the positioning area consisted of these four reference points is defined as the subpositioning area. Since the logarithmic RSSD measurements and the location of the four reference points are obtained, four hyperplane equations in matrix form for i-th AP combination are given by

$$\boldsymbol{A} \cdot \boldsymbol{K} = \boldsymbol{C}, \tag{9}$$

where

$$\boldsymbol{A} = \begin{bmatrix} x_1 & y_1 & \widetilde{R}_{i,1} \\ x_2 & y_2 & \widetilde{R}_{i,2} \\ x_3 & y_3 & \widetilde{R}_{i,3} \\ x_4 & y_4 & \widetilde{R}_{i,4} \end{bmatrix},$$

$$\boldsymbol{K} = \begin{bmatrix} k_{x,i} \\ k_{y,i} \\ k_{p,i} \end{bmatrix}, \tag{10}$$

$$\boldsymbol{C} = \begin{bmatrix} 1 \\ 1 \\ 1 \\ 1 \end{bmatrix},$$

where $k_{x,i}$, $k_{y,i}$, and $k_{p,i}$ are coefficients of the hyperplane equation corresponding to i-th AP combination, (x_j, y_j) (j=1, 2, 3, 4) is the location coordinate of the reference point, and $\widetilde{R}_{i,j}$ is the mean logarithmic RSSD measurement of j-th reference point from i-th AP combination. According to (10), the coefficients can be calculated by $\boldsymbol{K} = (\boldsymbol{A}^T \cdot \boldsymbol{A})^{-1} \cdot \boldsymbol{A}^T \cdot \boldsymbol{C}$. Thus, the relationship between the location coordinates and the i-th logarithmic RSSD within the choosing subpositioning area is obtained. Now that the subpositioning area of the URT has been determined, R can be replaced by the real-time RSSD of the positioning target and the relationship can be expressed by

$$k_{x,i} x + k_{y,i} y + k_{p,i} R_i = 1, \tag{11}$$

where R_i is the RSSD variable node of i-th AP combination. The other mathematical relationships related to different AP combinations can be obtained by the same method.

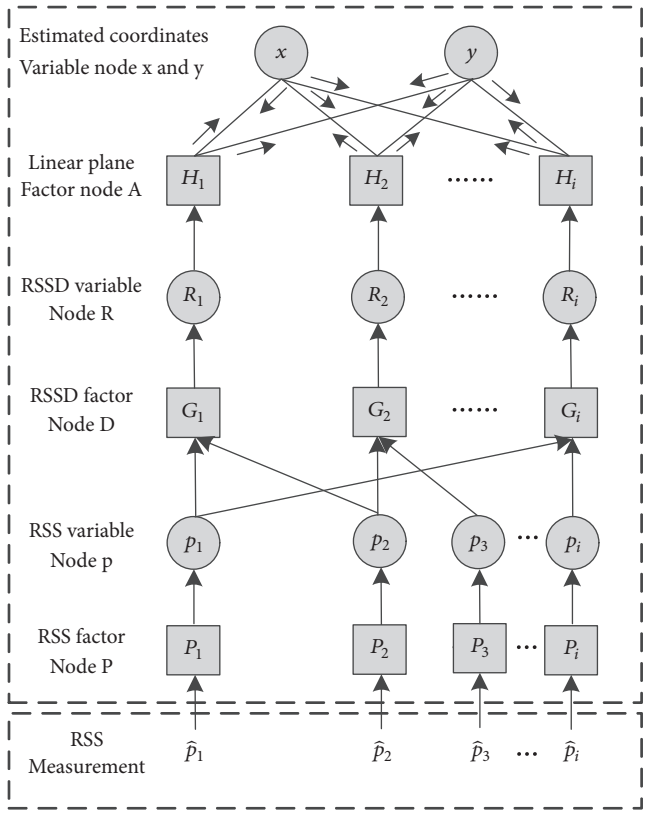

Figure 3: RSSD-based factor graph model.

3. Proposed RSSD-WLSFG Algorithm

3.1. RSSD-Based WLSFG Model. Actually, the RSSD measurement variances of different reference points are various due to the changing scenario, multipath effect, measuring position, and so on. In order to obtain a more accurate local relationship between location coordinates and RSSD, a new RSSD-based WLSFG model is proposed in this paper. First, we use RSSD-4NN approach to determine the subpositioning area from the reference points and utilize LS method to obtain the relationship between the coordinates (x_j, y_j) and the measured RSSD $(\widetilde{R}_{i,j})$, which is expressed by

$$k_{x,i}x_j + k_{y,i}y_j + k_{p,i}\widetilde{R}_{i,j} = 1. \tag{12}$$

From (9), the coefficients of (12) can be obtained by LS method. Second, we use (x_j, y_j) to calculate the estimated logarithmic RSSD $(\widetilde{R}'_{i,j})$ of j-th reference point from i-th AP combination according to (12) and the stochastic error of RSSD between the measured value and estimated value is given by

$$E_{i,j} = \widetilde{R}_{i,j} - \widetilde{R}'_{i,j}, \tag{13}$$

where $E_{i,j}$ is the stochastic error between the measured value and the estimated value of j-th reference point from i-th AP combination. Thus, the weighted matrix constructed with the stochastic errors is given by

$$\boldsymbol{W} = \boldsymbol{D}\boldsymbol{D}^T = \begin{bmatrix} E_{i,1}^2 & 0 & 0 & 0 \\ 0 & E_{i,2}^2 & 0 & 0 \\ 0 & 0 & E_{i,3}^2 & 0 \\ 0 & 0 & 0 & E_{i,4}^2 \end{bmatrix}, \tag{14}$$

where

$$\boldsymbol{D} = \begin{bmatrix} \sqrt{E_{i,1}^2} & 0 & 0 & 0 \\ 0 & \sqrt{E_{i,2}^2} & 0 & 0 \\ 0 & 0 & \sqrt{E_{i,3}^2} & 0 \\ 0 & 0 & 0 & \sqrt{E_{i,4}^2} \end{bmatrix},$$

$$\boldsymbol{D}^{-1} = \begin{bmatrix} \sqrt{E_{i,1}^2}^{-1} & 0 & 0 & 0 \\ 0 & \sqrt{E_{i,2}^2}^{-1} & 0 & 0 \\ 0 & 0 & \sqrt{E_{i,3}^2}^{-1} & 0 \\ 0 & 0 & 0 & \sqrt{E_{i,4}^2}^{-1} \end{bmatrix}. \tag{15}$$

If both sides of (9) are multiplied by $\boldsymbol{D}^{-1}$, we can obtain a new hyperplane equation expressed by

$$\boldsymbol{D}^{-1} \cdot \boldsymbol{A} \cdot \boldsymbol{K} = \boldsymbol{D}^{-1} \cdot \boldsymbol{C} \tag{16}$$

Here, coefficients of the new hyperplane equation can be calculated by the LS method given by

$$\boldsymbol{K}' = \left(\boldsymbol{A}^T \cdot \boldsymbol{W}^{-1} \cdot \boldsymbol{A}\right)^{-1} \cdot \boldsymbol{A}^T \cdot \boldsymbol{W}^{-1} \cdot \boldsymbol{C}, \tag{17}$$

where $\boldsymbol{K}' = \left[k'_{x,i} \;\; k'_{y,i} \;\; k'_{p,i}\right]^T$ is the coefficient matrix of the new hyperplane equation. Thus, the new relationship between the coordinate variable node (x, y) and the RSSD variable node R_i within the choosing subpositioning area is obtained, which is given by

$$k'_{x,i}x + k'_{y,i}y + k'_{p,i}R_i = 1. \tag{18}$$

The other hyperplane equations corresponding to different AP combinations can be obtained by using the same process above.

3.2. Soft-Information Calculation and Iteration Process. According to the sum-product algorithm, this section introduces how to calculate soft-information and deduces the iteration process. The initial soft-information passing from the variable nodes x and y to factor node H_i should be calculated at first. According to the sum-product algorithm, $SI(x, H_i)$ and $SI(y, H_i)$ are given by

$$SI\left(x, H_i\right) = \prod_{l \neq i}^{n} \left(H_l, x\right), \tag{19}$$

$$SI\left(y, H_i\right) = \prod_{l \neq i}^{n} \left(H_l, y\right). \tag{20}$$

Taking $SI(x, H_i)$ for example, its mean and variance can be calculated by

$$m_{x,H_i} = \sigma^2_{x,H_i} \left(\sum_{l \neq i}^{n} \frac{m_{H_l,x}}{\sigma^2_{H_l,x}}\right), \tag{21}$$

$$\sigma^2_{x,H_i} = \frac{1}{\left(\sum_{l \neq i}^{n} \left(1/\sigma^2_{H_l,x}\right)\right)} \tag{22}$$

In the same way, the soft-information $SI(y, H_i)$ can also be obtained. From (18), the soft-information $SI(H_i, x)$ transported from the factor node H_i to variable node x can be obtained by

$$m_{H_i,x} = \frac{\left(1 - k'_{y,i}m_{y,H_i} - k'_{p,i}m_{R_i,H_i}\right)}{k'_{x,i}}, \tag{23}$$

$$\sigma^2_{H_i,x} = \frac{\left(k'^2_{y,i}\sigma^2_{y,H_i} + k'^2_{p,i}\sigma^2_{R_i,H_i}\right)}{k'^2_{x,i}}. \tag{24}$$

Then, the soft-information $SI(H_i, y)$ can be calculated with the similar manner. The soft-information transported from the variable node R_i to factor H_i is equal to the factor node G_i to variable node R_i, where $m_{R_i,H_i} = m_{G_i,R_i}$ and $\sigma^2_{R_i,H_i} = \sigma^2_{G_i,R_i}$. From (7), the soft-information $SI(G_i, R_i)$ is calculated by

$$m_{G_i,R_i} = m_{p_i,G_i} - m_{p_1,G_i}, \tag{25}$$

$$\sigma^2_{G_i,R_i} = \sigma^2_{p_i,G_i} + \sigma^2_{p_1,G_i}. \tag{26}$$

The factor nodes P_1 and P_i directly transports the soft-information to node G_i, where $m_{p_1,G_i} = m_{P_1,p_1}$, $\sigma^2_{p_1,G_i} = \sigma^2_{P_1,p_1}$ and $m_{p_i,G_i} = m_{P_i,p_i}$, and $\sigma^2_{p_i,G_i} = \sigma^2_{P_i,p_i}$, respectively. According to (6), $SI(P_1, p_1)$ and $SI(P_i, p_i)$ can be directly obtained. In the same way, the transported soft-information of other AP combinations can also be obtained.

As mentioned above, all the soft-information has been calculated with the sum-product algorithm and the entire iteration process will be repeated until the estimated location of target is obtained. Finally, the soft-information of $SI(x)$ and $SI(y)$ can be updated by

$$m_x = \sigma^2_x \cdot \left(\sum_{i=1}^{n} \frac{m_{H_i,x}}{\sigma^2_{H_i,x}}\right), \tag{27}$$

$$\sigma^2_x = \frac{1}{\left(\sum_{i=1}^{n} \left(1/\sigma^2_{H_i,x}\right)\right)}, \tag{28}$$

$$m_y = \sigma^2_y \cdot \left(\sum_{i=1}^{n} \frac{m_{H_i,y}}{\sigma^2_{H_i,y}}\right), \tag{29}$$

$$\sigma^2_y = \frac{1}{\left(\sum_{i=1}^{n} \left(1/\sigma^2_{H_i,y}\right)\right)}. \tag{30}$$

From (27) and (29), the estimated location of the URT is determined by m_x and m_y. For better understanding, we summarize the entire iteration process as shown in Table 1.

4. Simulation and Analysis

To demonstrate the performance of proposed RSSD-WLSFG algorithm, the computer simulations of different algorithms are conducted on the platform of MATLAB2014a. The simulation scenario consists of 100 random target locations, 4 APs, and a positioning area of 100 m × 100 m. Here, we chose a well-known and easily implemented logarithmic shadowing model [20] to generate the random RSS measurements, which is expressed by

$$P\left(d_{i,j}\right) = P\left(d_0\right) - 10 \cdot \alpha \cdot \log_{10}\left(\frac{d_{i,j}}{d_0}\right) + \chi_j, \tag{31}$$

where $d_{i,j}$ is the distance between j-th reference point and i-th AP, d_0 is the reference distance, $P(d_0)$ is the RSS in decibel at the reference d_0, $P(d_{i,j})$ is the RSS of j-th reference point from i-th AP, α is path loss exponent, and χ_j represents the variance of the RSS measurements obeying zero-mean Gaussian distribution ($\chi_j \sim N(0, \sigma^2_{\chi_j})$). Then, the

Table 1: The soft-information processing of each node in Figure 3.

$SI(a,b)$	Inputs	Outputs
$SI(P_i, p_i)$	$(\widehat{p}_i, 0)$	$(m_{P_i,p_i}, \sigma^2_{P_i,p_i})$
$SI(p_i, G_i)$	$(m_{P_i,p_i}, \sigma^2_{P_i,p_i})$	$(m_{p_i,G_i}, \sigma^2_{p_i,G_i})$
$SI(G_i, R_i)$	$(m_{p_i,G_i}, \sigma^2_{p_i,G_i}), (m_{p_1,G_i}, \sigma^2_{p_1,G_i})$	$m_{G_i,R_i} = m_{p_i,G_i} - m_{p_1,G_i}, \sigma^2_{G_i,R_i} = \sigma^2_{p_i,G_i} + \sigma^2_{p_1,G_i}$
$SI(R_i, H_i)$	$(m_{G_i,R_i}, \sigma^2_{G_i,R_i})$	$m_{R_i,H_i} = m_{G_i,R_i}, \sigma^2_{R_i,H_i} = \sigma^2_{G_i,R_i}$
$SI(H_i, x)$	$(m_{R_i,H_i}, \sigma^2_{R_i,H_i}), (m_{y_i,H_i}, \sigma^2_{y_i,H_i})$	$m_{H_i,x} = \dfrac{(1 - k'_{y,i} m_{y,H_i} - k'_{p,i} m_{R_i,H_i})}{k'_{x,i}}$, $\sigma^2_{H_i,x} = \dfrac{(k'^2_{y,i}\sigma^2_{y,H_i} + k'^2_{p,i}\sigma^2_{R_i,H_i})}{k'^2_{x,i}}$
$SI(H_i, y)$	$(m_{R_i,H_i}, \sigma^2_{R_i,H_i}), (m_{x_i,H_i}, \sigma^2_{x_i,H_i})$	$m_{H_i,y} = \dfrac{(1 - k'_{x,i} m_{x,H_i} - k'_{p,i} m_{R_i,H_i})}{k'_{y,i}}$, $\sigma^2_{H_i,y} = \dfrac{(k'^2_{x,i}\sigma^2_{x,H_i} + k'^2_{p,i}\sigma^2_{R_i,H_i})}{k'^2_{y,i}}$
$SI(x, H_i)$	$(m_{H_l,x}, \sigma^2_{H_l,x})$	$m_{x,H_i} = \sigma^2_{x,H_i}\left(\sum_{l\neq i}^{n} \dfrac{m_{H_l,x}}{\sigma^2_{H_l,x}}\right)$, $\sigma^2_{x,H_i} = \dfrac{1}{\left(\sum_{l\neq i}^{n}\left(1/\sigma^2_{H_l,x}\right)\right)}$
$SI(y, H_i)$	$(m_{H_l,y}, \sigma^2_{H_l,y})$	$m_{y,H_i} = \sigma^2_{y,H_i}\left(\sum_{l\neq i}^{n} \dfrac{m_{H_l,y}}{\sigma^2_{H_l,y}}\right)$, $\sigma^2_{y,H_i} = \dfrac{1}{\left(\sum_{l\neq i}^{n}\left(1/\sigma^2_{H_l,y}\right)\right)}$
$SI(x)$	$(m_{H_i,x}, \sigma^2_{H_i,x})$	$m_x = \sigma^2_x \cdot \left(\sum_{i=1}^{n} \dfrac{m_{H_i,x}}{\sigma^2_{H_i,x}}\right)$, $\sigma^2_x = \dfrac{1}{(\sum_{i=1}^{n}(1/\sigma^2_{H_i,x}))}$
$SI(y)$	$(m_{H_i,y}, \sigma^2_{H_i,y})$	$m_y = \sigma^2_y \cdot \left(\sum_{i=1}^{n} \dfrac{m_{H_i,y}}{\sigma^2_{H_i,y}}\right)$, $\sigma^2_y = \dfrac{1}{\left(\sum_{i=1}^{n}\left(1/\sigma^2_{H_i,y}\right)\right)}$

random RSS measurement $\widetilde{p}_{i,j}$ can be considered as Gaussian distribution ($\widetilde{p}_{i,j} \sim N(P(d_0) - 10 \cdot \alpha \cdot \log_{10}(d_{i,j}/d_0), \sigma^2_{\chi_j})$). Due to the multipath effect, small scale fading, system hardware influence, and measurement error, $\sigma^2_{\chi_j}$ is not the same at different reference points. We denote $(\sigma^2_{\chi_1}, \sigma^2_{\chi_2}, \ldots, \sigma^2_{\chi_j}) \in \sigma^2_{\chi}$, and the variable σ^2_{χ} is assumed as Gaussian distribution ($\sigma^2_{\chi} \sim N(m_{\chi}, \sigma^2_s)$). Here, we define that m_{χ} is the mean variance of all reference points, where $m_{\chi} = (\sigma^2_{\chi_1} + \sigma^2_{\chi_2} + \cdots + \sigma^2_{\chi_q})/q$ and q is the number of reference point. The typical values for d_0=1 m, $P(d_0)$=10 dB, and α =1.8 are as [17]. To verify the positioning performance of proposed RSSD-WLSFG algorithm, m_{χ} varies with 5 dB interval between 5 dB and 30 dB and σ^2_s is fixed at 5 dB in our simulation. The simulated RSS measurement data of off-line database and online positioning target can be obtained with the method as in [17]. At first, 100 single URT locations are randomly chosen from the positioning area of 100 m × 100 m and the location coordinates of 4 APs identified with solid "Δ" mark are (17,25) m, (43,75) m, (67,75) m, and (83,25) m, respectively. The localization results of proposed RSSD-WLSFG algorithm are shown in Figure 4. Figure 5 shows that the root mean square error (RMSE) of the proposed algorithm rapidly decreases with the increasing number of the iterations. When the number of iteration approaches 10, the RMSE tends to be stable at 1.35m. It can be seen that the proposed algorithm has fast convergence. Next, taking the different variances of RSS measurements into account, the RSSD-4NN and RSSD-FG algorithms are selected to compare with the proposed algorithm in the case of different grid distances and AP numbers. First, three algorithms are simulated with different grid distances (1.5 m, 2 m, and 3 m) and 4 APs to evaluate the positioning performance of these algorithms. From the simulation results in Figure 6, it can be obtained that the proposed RSSD-WLSFG algorithm has a higher positioning accuracy than the RSSD-FG algorithm and RSSD-KNN algorithm in the case of three different grid distances. Taking m_{χ} = 20 dB and d = 1.5m as an example, the RMSE for each algorithm is 1.31 m for RSSD-WLSFG, 1.43 m for RSSD-FG, and 1.82 m for RSSD-4NN. It can be seen from the trend of the curves that the higher positioning accuracy can be achieved with the smaller grid distance. For RSSD-WLSFG and RSSD-FG algorithms, this is mainly because the smaller subpositioning area, which is caused by the smaller grid distance, is more corresponding to the requirement of hyperplane approximation with shadowing area. For RSSD-4NN algorithm, the larger grid distance leads to fewer reference points in the database, and it increases the distance between the selected reference points and the positioning target so as to reduce the accuracy.

Second, we explore the influence of different AP numbers on the positioning accuracy. It can be found that the RMSE becomes smaller when the number of AP increases as shown in Figure 7. Compared with the RSSD-FG and RSSD-4NN algorithms, the RMSE of proposed RSSD-WLSFG algorithm with the corresponding AP numbers is the smallest. However, with the increasing AP numbers, positioning accuracy is not unlimited to be enhanced. The RMSE with four APs is 1.41 m, and it is similar to that with five APs which is 1.37 m. Similarly, the RMSE curves of four APs are also very close

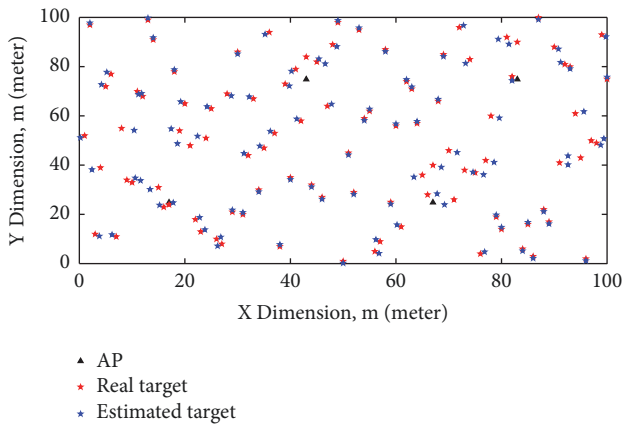

Figure 4: Localization results of 100 random test targets with 4 APs in positioning area 100 m × 100 m, 1.5m grid distance, and m_χ = 20 dB.

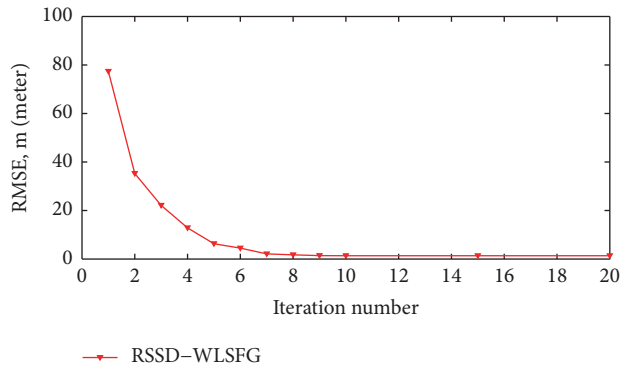

Figure 5: Root mean square error of proposed RSSD-WLSFG algorithm with the iteration changing from 1 to 20 times, 1.5 m grid distance, 4 APs, and m_χ = 25 dB.

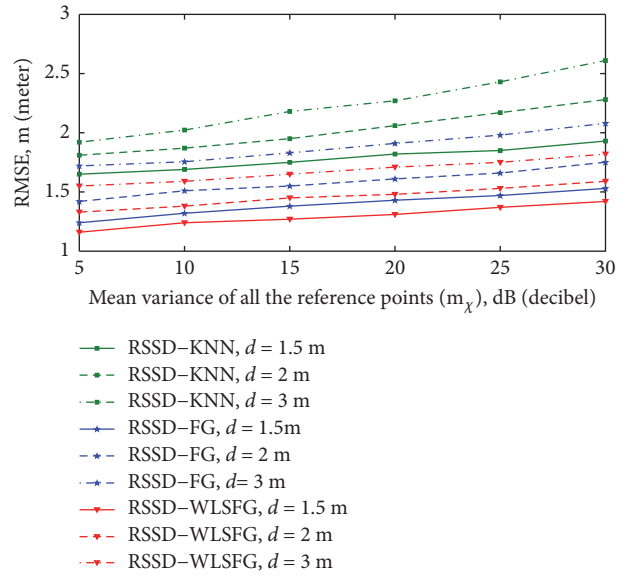

Figure 6: Root mean square error comparison among RSSD-4NN, RSSD-FG, and proposed RSSD-WLSFG with 1.5 m, 2 m, and 3 m grid distances, respectively and 4 APs.

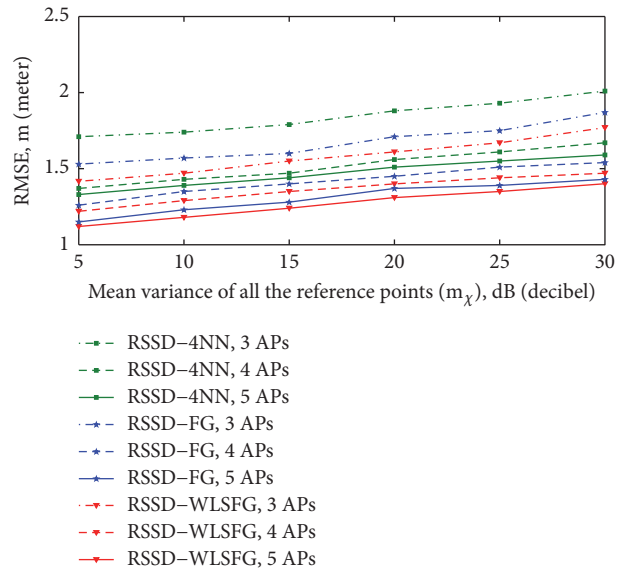

Figure 7: Root mean square error comparison among RSSD-4NN, RSSD-FG, and proposed RSSD-WLSFG with 3 APs, 4 APs, and 5 APs, respectively, and 1.5 m grid distance.

to RMSE curves of five APs. Moreover, even with the use of four APs, the proposed algorithm still has a higher accuracy than the conventional RSSD-4NN algorithm with five APs. Due to hyperplane approximation, the optimal number of AP is four APs with hyperplane natural shape consisting of four edge sharp points. Therefore, the square shape of reference points is superior to circles, rectangles, and other shapes. The RSS-FG technique without using the square shape is due to the real environment of the road [21]. Above all, we utilize four APs to meet the detection requirements for the URT.

5. Experiment Results and Discussions

Finally, the proposed RSSD-WLSFG algorithm is validated by field test, which is located on the first floor of the National Radio Monitoring Center, Beijing. The test field consists of an office and its adjacent corridor with an area of 14.4 m × 8.4 m and 14.4m × 2.1 m, respectively. The total area of the test field is 151.2 square meters. In addition, there are four windows on one wall of the office and two doors on the other wall adjacent to the corridor and there are no partitions or compartments. The main items in the office are six rows of desks, chairs, and computers and human beings are free to enter and leave frequently throughout the whole test. The layout of test field is as shown in Figure 8.

In the offline fingerprint database establishment phase, the positioning area is divided into two kinds of grid distances: 1.5m and 2m. Four SA44B (Signal Hound Co. Ltd.) signal receivers are used as APs to collect the RSS measurements. The number and layout of the APs are selected with two types, which labels are "1#" and "2#" as shown in Figure 8. Four APs labeled "1#" are deployed in the office where they are at (3,2) m, (8,5) m, (3,9) m, and (8,12) m, respectively. Three APs locations labeled "2#" are (2,7)

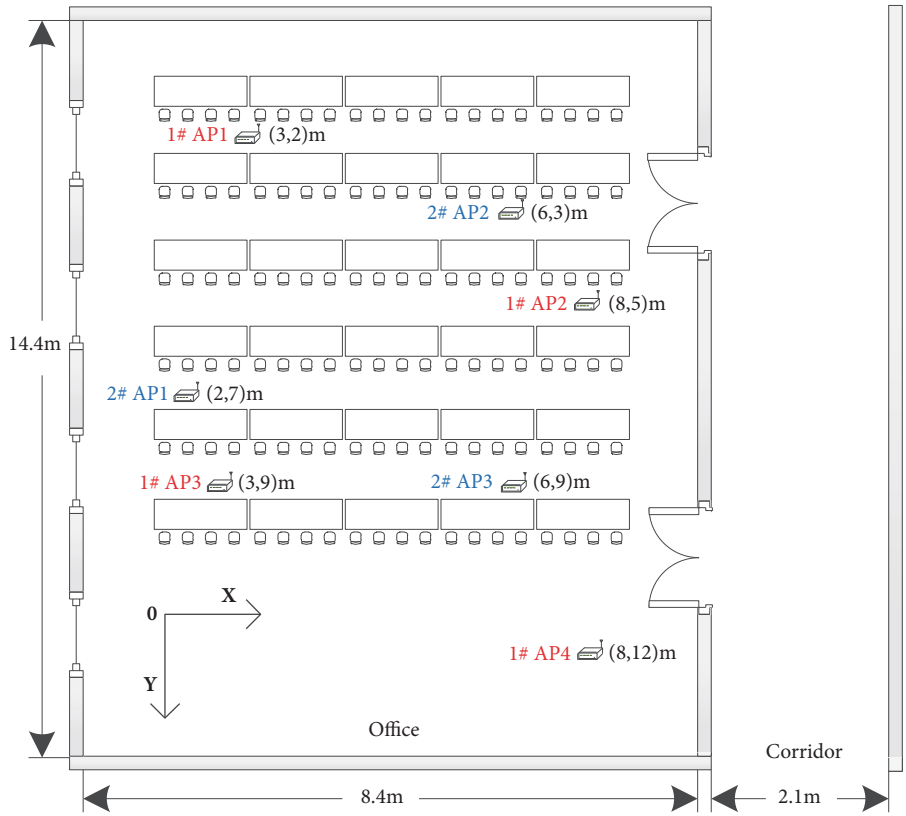

Figure 8: Layout of the test field.

m, (6,3) m, and (6,9) m, respectively. In this experiment, the radio transmitter TFG6300 (SUING Co. Ltd.) used to establish the fingerprint database and be as the URT is adjustable in transmitting "frequency/strength." In order to better prove the adaptability of the proposed RSSD-WLSG algorithm for different frequency and strength, we choose "1 GHz/ 20 dB" offline database and "300 MHz/ 13 dB" URT in the test. Here, the RSS measurements of each reference point in the fingerprint database are obtained by averaging 100 RSS samples from each AP. In the positioning area, 50 testing points were selected for localization test.

The mean location errors and cumulative distribution function (CDF) of location errors are used as the key evaluation indicators to compare the performance of RSSD-WLSFG, RSSD-FG, and RSSD-4NN. The mean location errors are characterized by the average deviation value of all the estimated positioning targets that compared with the real location, and CDF represents the distribution of the location errors expressed as percentage. First, the test comparison of different grid distances (1.5 m and 2 m) among the three algorithms is conducted in the positioning area. The mean location errors of different algorithms with four APs are as shown in Table 2. When the grid distance is 1.5 m, the mean location error by the proposed RSSD-WLSFG algorithm is 1.06m. In comparison, the mean location errors of RSSD-FG and RSSD-4NN are 1.24 m and 1.42 m, respectively. With the grid distance increasing to 2 m, the mean location errors of RSSD-4NN, RSSD-LSFG, and RSSD-WLSFG are 1.72 m, 1.45 m, and 1.27 m, respectively. The CDF of RSSD-4NN, RSSD-FG, and RSSD-WLSFG is as shown in Figure 9. When the grid distance is 1.5 m or 2 m, the number of qualified testing points of the proposed algorithm within different location errors is larger than that of the other two algorithms. Considering the location error within 1.5 m, the CDF for each algorithm is 52 percent for RSSD-4NN, 66 percent for RSSD-FG, and 72 percent for RSSD-WLSFG when the grid distance is 1.5 m. The CDF of RSSD-4NN, RSSD-FG, and RSSD-WLSFG is 36 percent, 54 percent and 62 percent, respectively, when the grid distance is 2 m and the location error within 1.5 m. The results show that the positioning accuracy of proposed RSSD-WLSFG algorithm is better than RSSD-FG and RSSD-4NN no matter the grid distance being 1.5 m or 2 m.

Next, we explore the effect of the number of AP on the positioning accuracy through experiments. The 1.5 m grid distance is selected to evaluate the positioning performance of different algorithms when the number of APs is three and four, respectively. The comparison of the mean location errors among different algorithms with 1.5 m grid distance is as shown in Table 3. The mean location errors of RSSD-4NN, RSSD-FG, and RSSD-WLSFG algorithms are 1.79 m, 1.55 m, and 1.31 m, respectively, when utilizing 3 APs. It can be observed from the comparison of experimental results that the mean location errors of three algorithms are 1.36 m, 1.19 m, and 1.09 m, respectively, with 4 APs. Figure 10 shows the CDF comparison of location errors with different APs. The CDF of RSSD-4NN, RSSD-FG, and RSSD-WLSFG is 42

Table 2: Mean location errors of different grid distances with 4 APs.

Grid distance	RSSD-4NN	RSSD-FG	RSSD-WLSFG
1.5 m	1.42 m	1.24 m	1.06 m
2 m	1.72 m	1.45 m	1.27 m

Table 3: Mean location errors of different APs with 1.5 m grid distance.

AP numbers	RSSD-4NN	RSSD-FG	RSSD-WLSFG
3 APs	1.79 m	1.55 m	1.31 m
4 APs	1.36 m	1.19 m	1.09 m

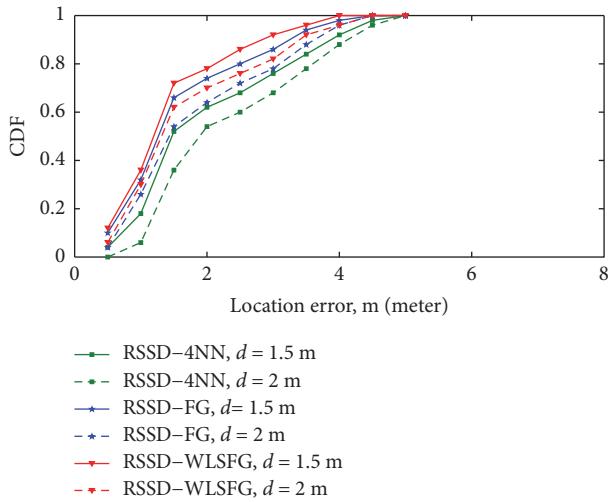

Figure 9: CDF comparison of location errors with 1.5 m and 2 m grid distances, respectively, and 4 APs.

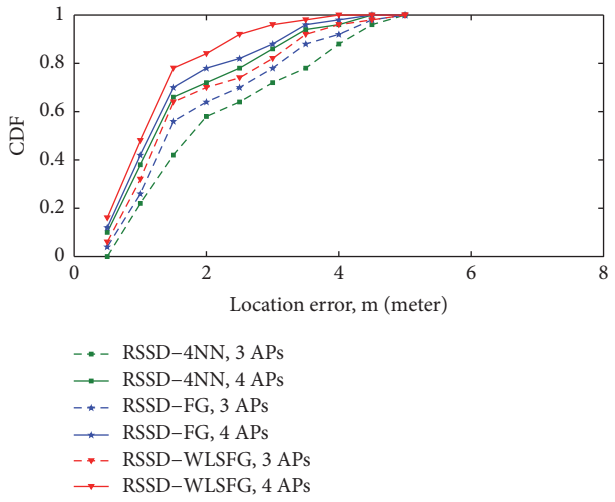

Figure 10: CDF comparison of location error with 3 and 4 APs, respectively, and 1.5 m grid distance.

percent, 56 percent, and 62 percent, respectively, when the number of AP is three and the location error within 1.5 m. When the number of AP increases to four, the CDF for each algorithm is 62 percent for RSSD-4NN, 68 percent for RSSD-FG, and 72 percent for RSSD-WLSFG when the location error is within 1.5 m. The results demonstrate that the increase of the number of AP can improve the positioning accuracy. In the case of different numbers of AP, the positioning performance of proposed algorithm is superior to the other two algorithms. The above experimental results show that the proposed RSSD-WLSFG algorithm has a higher positioning accuracy than RSSD-4NN and RSSD-FG in different grid distances and AP numbers.

6. Conclusions

For the localization requirement of the URT in radio management, this paper has proposed a new RSSD-WLSFG algorithm to achieve more accurate detection of an URT. With the Gaussian assumption of the RSS measurements, an enhanced RSSD-based FG model is established with WLS method to eliminate the influence from the variance diversity of reference points. Through weight calculation, the relationship between the RSSD measured value and the location coordinates is more reasonable and accurate, which effectively mitigates the error caused by the reference point with larger variance of RSSD measurement. The soft-information calculation and iteration process of the proposed RSSD-WLSFG algorithm are deduced by using the sum-product algorithm. In addition, considering the main factors affecting the accuracy of fingerprint positioning technology in practical application, the positioning performance of the proposed algorithm under different grid distances and different AP numbers is explored, respectively. A large number of experimental results show that the proposed method has better positioning performance than the RSSD-FG and RSSD-4NN algorithms. It not only meets the positioning requirements but also has a better application prospect. The effect of AP's layout and detection of multi-URTs will be involved in our future research.

Data Availability

The data used to support the findings of this study are available from the corresponding author upon request.

Conflicts of Interest

The authors declare that they have no conflicts of interest.

Acknowledgments

The authors gratefully acknowledge the support from the Ministry of Industry and Information Technology of the People's Republic of China (CN) (No. 12-MC-KY-14).

References

[1] M. Bocquet, C. Loyez, and A. Benlarbi-Delaï, "Using enhanced-TDOA measurement for indoor positioning," *IEEE Microwave and Wireless Components Letters*, vol. 15, no. 10, pp. 612–614, 2005.

[2] H. G. Yu, G. M. Huang, J. Gao, and B. Liu, "An efficient constrained weighted least squares algorithm for moving source location using TDOA and FDOA measurements," *IEEE Transactions on Wireless Communications*, vol. 11, no. 1, pp. 44–47, 2012.

[3] J. Talvitie, M. Renfors, and E. S. Lohan, "Distance-based interpolation and extrapolation methods for RSS-based localization with indoor wireless signals," *IEEE Transactions on Vehicular Technology*, vol. 64, no. 4, pp. 1340–1353, 2015.

[4] P. N. Pathirana, S. W. Ekanayake, and A. V. Savkin, "Fusion based 3D tracking of mobile transmitters via robust set-valued state estimation with RSS measurements," *IEEE Communications Letters*, vol. 15, no. 5, pp. 554–556, 2011.

[5] Y. Wang and K. C. Ho, "An asymptotically efficient estimator in closed-form for 3-D AOA localization using a sensor network," *IEEE Transactions on Wireless Communications*, vol. 14, no. 12, pp. 6524–6535, 2015.

[6] S. Tomic, M. Beko, and R. Dinis, "Distributed RSS-AoA Based Localization with Unknown Transmit Powers," *IEEE Wireless Communications Letters*, vol. 5, no. 4, pp. 392–395, 2016.

[7] Y. Wang, Y. Wu, D. Wang, and Y. Shen, "TDOA and FDOA based source localisation via importance sampling," *IET Signal Processing*, vol. 12, no. 7, pp. 917–929, 2018.

[8] M. T. Hoang, Y. Zhu, B. Yuen et al., "A Soft Range Limited K-Nearest Neighbors Algorithm for Indoor Localization Enhancement," *IEEE Sensors Journal*, vol. 18, no. 24, pp. 10208–10216, 2018.

[9] P. Bahl and V. N. Padmanabhan, "RADAR: an in-building RF-based user location and tracking system," in *Proceedings of the 19th Annual Joint Conference of the IEEE Computer and Communications Societies (IEEE INFOCOM '00)*, vol. 2, pp. 775–784, Tel Aviv, Israel, 2000.

[10] L. M. Ni, Y. H. Liu, Y. C. Lau, and A. P. Patil, "LANDMARC: indoor location sensing using active RFID," in *Proceedings of the 1st IEEE International Conference on Pervasive Computing and Communications (PerCom '03)*, Fort Worth, Tex, USA, 2003.

[11] A. K. M. Mahtab Hossain, Y. Jin, W. Soh, and H. N. Van, "SSD: a robust RF location fingerprint addressing mobile devices' heterogeneity," *IEEE Transactions on Mobile Computing*, vol. 12, no. 1, pp. 65–77, 2013.

[12] X. Lin, H. Wang, and L. Wang, "Cognitive cooperative location algorithm research based on RSSD and TDOA technology," *Journal of Signal Processing*, vol. 32, no. 8, pp. 931–936, 2016.

[13] J.-C. Chen, Y.-C. Wang, C.-S. Maa, and J.-T. Chen, "Network-side mobile position location using factor graphs," *IEEE Transactions on Wireless Communications*, vol. 5, no. 10, pp. 2696–2704, 2006.

[14] H.-L. Jhi, J.-C. Chen, C.-H. Lin, and C.-T. Huang, "A factor-graph-based TOA location estimator," *IEEE Transactions on Wireless Communications*, vol. 11, no. 5, pp. 1764–1773, 2012.

[15] C. Mensing and S. Plass, "Positioning based on factor graphs," *EURASIP Journal on Advances in Signal Processing*, vol. 1, no. 4, pp. 1–11, 2007.

[16] M. R. K. Aziz, *Factor Graph-Based Geolocation Techniques for Position Detection of Unknown Radio Wave Emitter [PhD. thesis]*, Japan Advanced Institute of Science and Technology, JAIST Press, 2016.

[17] C.-T. Huang, C.-H. Wu, Y.-N. Lee, and J.-T. Chen, "A novel indoor RSS-based position location algorithm using factor graphs," *IEEE Transactions on Wireless Communications*, vol. 8, no. 6, pp. 3050–3058, 2009.

[18] M. R. K. Aziz, K. Anwar, and T. Matsumoto, "DRSS-based factor graph geolocation technique for position detection of unknown radio emitter," in *Proceedings of the 22th European Wireless Conference*, pp. 300–305, Oulu, Finland, 2016.

[19] F. R. Kschischang, B. J. Frey, and H.-A. Loeliger, "Factor graphs and the sum-product algorithm," *IEEE Transactions on Information Theory*, vol. 47, no. 2, pp. 498–519, 2001.

[20] T. S. Rappaport, *Wireless Communication-Principles and Practice*, Prentice Hall, 1996.

[21] M. R. Aziz, S. N. Karimah, N. Yoshio, K. Anwar, and T. Matsumoto, "Achieving accurate geo-location detection using joint RSS-DOA factor graph technique," in *Proceedings of the 2016 10th International Conference on Telecommunication Systems Services and Applications (TSSA '16)*, pp. 1–6, Denpasar, Indonesia, 2016.